Active control of thermoacoustic amplification in a thermo-acousto-electric engine

Come Olivier, Guillaume Penelet, Gaëlle Poignand, Pierrick Lotton

Active control of thermoacoustic amplification in a thermo-acousto-electric engine

Come Olivier, Guillaume Penelet, Gaelle Poignand, and Pierrick Lotton

Citation: Journal of Applied Physics **115**, 174905 (2014); doi: 10.1063/1.4874743
View online: http://dx.doi.org/10.1063/1.4874743
View Table of Contents: http://scitation.aip.org/content/aip/journal/jap/115/17?ver=pdfcov
Published by the AIP Publishing

Active control of thermoacoustic amplification in a thermo-acousto-electric engine

Come Olivier,[a] Guillaume Penelet, Gaelle Poignand, and Pierrick Lotton
Laboratoire d'Acoustique de l'Université du Maine, UMR CNRS 6613, Avenue Olivier Messiæn, 72085 LE MANS Cedex 9, France

(Received 19 December 2013; accepted 22 April 2014; published online 5 May 2014)

In this paper, a new approach is proposed to control the operation of a thermoacoustic Stirling electricity generator. This control basically consists in adding an additional acoustic source to the device, connected through a feedback loop to a reference microphone, a phase-shifter, and an audio amplifier. Experiments are performed to characterize the impact of the feedback loop (and especially that of the controlled phase-shift) on the overall efficiency of the thermal to electric energy conversion performed by the engine. It is demonstrated that this external forcing of thermoacoustic self-sustained oscillations strongly impacts the performance of the engine, and that it is possible under some circumstances to improve the efficiency of the thermo-electric transduction, compared to the one reached without active control. Applicability and further directions of investigation are also discussed. © *2014 AIP Publishing LLC*. [http://dx.doi.org/10.1063/1.4874743]

I. INTRODUCTION

Since the description by Sondhauss[1] of a tube singing when heated at its closed end, a renewal of interest occurred in the study of thermoacoustic oscillators as new kinds of heat engines. In the past three decades, the theoretical works by Rott[2] and the pioneering ideas of Ceperley,[3] Wheatley,[4] or Swift[5] led to an intense research activity in the field that gave rise to the development of various prototypes combining good efficiency with fundamental advantages such as simplicity and high reliability. One of these prototypes is the so-called ThermoAcoustic-Stirling Heat Engine (TASHE) built by Backhaus and Swift[6,7] in 1999, which demonstrated both high efficiency (up to 30%) and high power (up to 1 kW of acoustic power). A few years later, Backhaus *et al.*[8] developed another similar engine in which acoustical work is transformed into electrical energy via the coupling of the thermoacoustic oscillator to an electrodynamic linear alternator.

In this paper, the device under consideration (see Fig. 1) is a thermo-acousto-electric Stirling generator similar to the one developed by Backhaus *et al.*[8] It consists of a closed-loop waveguide containing the thermoacoustic core, and connected to the acoustic load (i.e., the electrodynamic alternator). The thermal to acoustic energy conversion relies on imposing a steep temperature gradient along a porous material, referred to as the regenerator, which gives rise to the onset of self-sustained acoustic oscillations.[5] The saturation of acoustic waves, and therefore the efficiency of thermoacoustic energy conversion, is controlled by several nonlinear effects. Among them is the thermoacoustic heat pumping, reducing the externally imposed temperature gradient,[2,9] as well as the generation of acoustic streaming[10–15] but also other nonlinear phenomena such as wave steepening,[16,17] minor losses,[18] or turbulence.[19] All of these phenomena contribute together to reducing the overall efficiency of the engine either by dissipating acoustic power or by modifying the temperature field in the heterogeneously heated part of the device. However, due to the complexity of the phenomena mentioned above (and also to the intricacy of heat transfer through the thermoacoustic core),[20,21] the available design tools[22,23] based on the linearization of the governing equations are not perfectly adequate to predict the steady-state operation of thermoacoustic engines (in both terms of wave amplitude and temperature distribution along the thermoacoustic core). As a result, researchers developing thermoacoustic hardware have used semi-empirical techniques in order to minimize or to counteract the nonlinear effects mentioned above. Most of these techniques consist in using passive elements to be added to the engines at strategic locations, such as tapered tubes,[7,24] flow straighteners,[7] jet pumps,[7] or membranes.[25] Apart from the flow straighteners, whose main role is to keep the flow laminar, the solutions mentioned above are used to control the temperature field, trying to minimize empirically the effects of heat convection by acoustic streaming.

The objective of this paper is to investigate another approach for the control of acoustic oscillations above the onset, which basically consists in trying to drive the autonomous oscillator by means of an external sound source (instead of trying to control heat transport through the thermoacoustic core). In the context of energetic applications, the main scope of this study is therefore to see if a small forcing of thermoacoustic oscillations can lead to an overall increase of the engine's efficiency. The external forcing of self-sustained oscillations has been investigated in many fields of science.[26] In particular, it has been explored in the field of thermoacoustics to study phase and frequency locking phenomena[27–30] or the quasiperiodic transition to chaos.[31] The possibility to increase the heat to sound energy conversion in an annular thermoacoustic engine by means of two auxiliary acoustic sources has also been demonstrated by Desjouy *et al.*[32]

[a]Author to whom correspondence should be addressed. Electronic mail: come.olivier@univ-lemans.fr

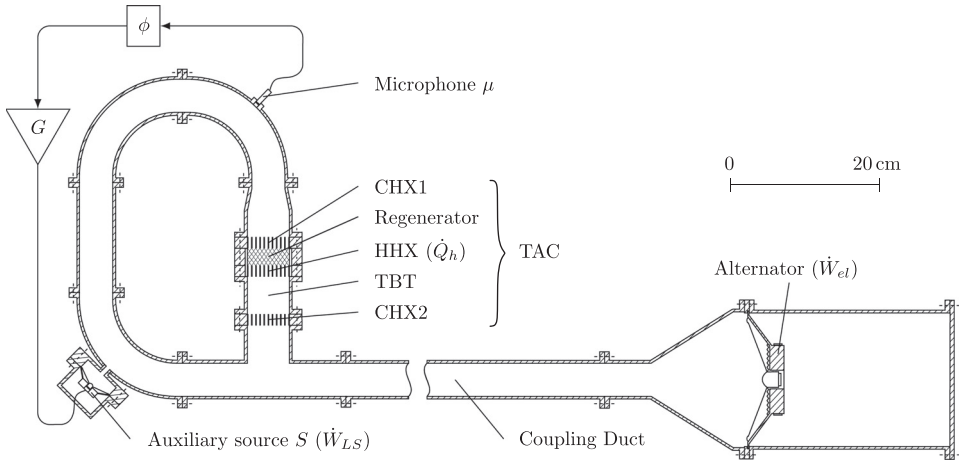

FIG. 1. Scale schematic of the thermo-acousto-electric engine used in this study. The torus-shaped part contains the TAC, mainly composed of the regenerator and heat exchangers. The closed loop waveguide is connected to the alternator via a coupling duct. The active control system is also presented schematically on the left: it consists of a feedback loop driving the auxiliary acoustic source. The reference pressure signal measured by the microphone μ is phase-shifted by a phase ϕ and amplified by a gain G to power the auxiliary source S.

The present study is actually a continuation of the latter works, in which both the thermoacoustic device and the active control method are different.

In Sec. II, a description of both the thermo-acousto-electric engine and the active control system (which basically consists of a single loudspeaker connected through a feedback loop to a reference microphone, a phase-shifter, and an audio amplifier) are provided. In Sec. III, experimental results are presented, which demonstrate that the appropriate tuning of the feedback loop enables to increase the engine's performance. Finally, a discussion is given in Sec. IV about the applicability of this active control process for energetic applications, as well as some enlightenment on the possible improvement of the presented results.

II. EXPERIMENTAL APPARATUS

A schematic of the prototype used in this study presented in Fig. 1: apart from the presence of a feedback loop to control thermoacoustic amplification, this system is comparable to the engine built by Backhaus *et al.*[8] It is mainly composed of a thermoacoustic core (TAC) connected through a closed-loop waveguide to the acoustic load that ends with an electrodynamic alternator. The operation of this engine consists in assigning a temperature difference ΔT_0 along the regenerator, which leads, above some threshold value, to the onset of self-sustained acoustic waves oscillating at the frequency f_o of the most unstable acoustic mode of the system.

The torus-shaped waveguide (unwrapped length: 1.12 m) contains the thermoacoustic core (inner radius: 28 mm, length: 11.8 cm), which is itself composed of two cold heat exchangers separated by a regenerator, a hot heat exchanger, and a thermal buffer tube (TBT). A first ambient heat exchanger (CHX1), made of a 15 mm-thick copper block drilled with 303 holes (inner diameter: 2 mm), is placed at the top of the core. Its porosity is 0.6. It is chilled by room-temperature water pumped from a tank and circulating in a circumferential groove through the shell. The central piece of the TAC is the regenerator. It consists of a 2.3 cm-long stack of stainless-steel wire-mesh screens. The diameter of the mesh wire is 32 μm. The porosity of the regenerator is evaluated to 0.69 and its hydraulic radius is 20 μm. The temperature gradient is imposed by the hot heat exchanger (HHX), below the regenerator, which consists of a 2.0 m-long and 3 mm-wide Nichrome ribbon inserted into a ceramic 0.9 mm-wide square-pores stack to form two perpendicular zigzags patterns covering a maximum of the cross section of the tube. This exchanger is 15 mm-long and its estimated porosity is 0.89. Electrical power is supplied by a DC-power supply (EX420R, 42 V, 10 A, Thurlby Thandar Instruments) and dissipated through the Nichrome ribbon. A resulting heat power up to $\dot{Q}_h = 180$ W is therefore provided through the HHX, leading to a gas temperature up to 700 °C. Both the hot heat exchanger and the regenerator are inserted into a tube of ceramic to thermally insulate them from the surrounding stainless steel walls and reduce the thermal leaks to the outside. To complete the TAC, a 5 cm-long duct provides a thermal buffer between the hot exchanger and the second cold heat exchanger CHX2, which is similar in all respects to CHX1. The remaining part of the closed loop waveguide (unwrapped length: 1 m, inner radius: 21 mm) connects both sides of the TAC and the acoustic load through a T-junction (as depicted in Fig. 1). The acoustic load consists of a straight coupling duct (length: 1.55 m, inner radius: 21 mm) connected to a conical duct (length: 12 cm) leading to the 18 cm-diameter electrodynamic loudspeaker—a Monacor SPH-170C—used here as an alternator. This loudspeaker has been chosen for its low resonance frequency ($f_s \simeq 38$ Hz) and its high force factor ($Bl \simeq 9$ Tm). It is loaded by a 4.3 l back cavity that acts as an acoustic compliance in order to match the impedances at the T-junction. The electrical power $\dot{W}_{el}$ generated by the alternator is measured by dissipating it in a resistor of resistance R_L across which the voltage is measured.

Two thermocouples are inserted in the middle of the two main heat exchangers (CHX1 and HHX) allowing the measurement of the temperature difference through the regenerator

$$\Delta T = T_{\mathrm{HHX}} - T_{\mathrm{CHX1}}. \tag{1}$$

The electroacoustic feedback loop used for the active control is also presented schematically in Fig. 1. It is composed of a microphone (μ) measuring the acoustic pressure close to the point of its highest amplitude in the engine. The microphone signal is phase-shifted with a phase-shift ϕ and amplified with an amplification gain G. This resulting signal

is used to power a small enclosed loudspeaker S (Visaton FRS 5), coupled to the engine by a 35.2 mm-long, 7 mm-diameter capillary duct. The coupling of the auxiliary source with the engine having a strong impact on the onset threshold of the engine, its location has been chosen in order to minimize that effect. The onset threshold in presence of the source has been predicted[23] to its minimum value around the chosen position (see Fig. 1), the required temperature difference growing rapidly away from this point. The current running through the speaker coil is evaluated by measuring the voltage across a small resistor mounted in series, giving access to the electric power $\dot{W}_{LS}$ supplied to the auxiliary source. The steady-state overall efficiency η of the engine is finally defined as the ratio of the outgoing to incoming electrical powers

$$\eta = \frac{\dot{W}_{el}}{\dot{Q}_h + \dot{W}_{LS}}. \tag{2}$$

Note that it is possible to measure the available acoustic power $\dot{W}_{ac}$ in the resonator with a two-microphone method,[33] which allows to quantify the acoustic to electric conversion efficiency $\eta_{alt} = \dot{W}_{el}/\dot{W}_{ac}$ of the alternator. It has been found to be constant $\eta_{alt} \simeq 0.41$ for the conditions of operation of the engine investigated hereafter in Sec. III. It is therefore a reasonable assumption to consider that the variations of the overall efficiency η are representative of the variations of the thermoacoustic conversion efficiency $\eta_{reg} = \dot{W}_{ac}/(\dot{Q}_h + \dot{W}_{LS})$ within the regenerator.

The complete device is filled with air at a moderate gauge pressure (typically, $P_0 = 5$ bars), and its onset temperature difference is $\Delta T_o < 300$ K when the alternator is loaded with an infinite resistance $R_L = \infty$. Its onset frequency f_o corresponds to the resonance frequency of the complete system, but is mostly governed by the quarter-wavelength resonator so that $f_o \simeq 40$ Hz. The resistance of the load applied to the alternator is chosen as $R_{L,opt} = 16.7\,\Omega$ to optimize η, so that $\eta_{max} \simeq 0.01$. The maximum output power produced by the engine is $\dot{W}_{el,max} \simeq 1\,W$. It is worth pointing out that, though it has been designed to operate close to its maximum efficiency, this prototype being a study model, priority has been put on its simplicity of manufacture and ease of use before its performances. Notably, because it operates with moderately pressurized air instead of highly pressurized Helium (a gas with better thermoacoustic properties and a higher power density due to pressurization), its overall efficiency and output power are limited. For both these reasons, the capabilities of this prototype are not comparable with those of the engines built by Backhaus and Swift.[6,7] Moreover, the performances mentioned above are those obtained without the electroacoustic feedback loop, the addition of which affects the performances (e.g., the onset threshold in presence of the feedback loop is circa 45 K more important than without it). This point will be discussed further in Sec. IV.

III. EXPERIMENTAL RESULTS

In the following, the influence of the electroacoustic feedback loop on the operation of the thermoacoustic engine is investigated. The study is conducted by measuring the output electrical power $\dot{W}_{el}$ as a function of the available control parameters, which are the input heat power $\dot{Q}_h$ and the two parameters controlling the feedback loop, namely, the phase shift ϕ and the amplification gain G.

The main objective is to quantify the effects of the feedback loop in the light of the reference results obtained without active control. Accordingly, the reference results (later on indicated by subscript $_0$) considered are those obtained when the auxiliary source is not powered (i.e., $G = 0$). The first quantity of interest is therefore the evolution of the overall efficiency $\eta(\dot{Q}_h, \phi, G)$, compared with the reference overall efficiency $\eta_0(\dot{Q}_h)$. The reference efficiency η_0 is to be found in Fig. 2, and it is measured to increase monotonously with $\dot{Q}_h$ up to approximately 0.6%. Another quantity of interest is the evolution of the temperature difference in the regenerator $\Delta T(\dot{Q}_h, \phi, G)$ in the same conditions. It is compared to the reference temperature difference $\Delta T_0(\dot{Q}_h)$ when the auxiliary source is not powered, which is also given in Fig. 2. Finally, the additional power produced thanks to the electroacoustic feedback loop $\Delta\dot{W}_{el} = \dot{W}_{el} - \dot{W}_{el0}$ should be compared to the power supplied to the control loudspeaker $\dot{W}_{LS}$.

A. Effect of phase-shift ϕ at fixed input heat power $\dot{Q}_h$ for various amplification gains G

At first, the input heat power is fixed to $\dot{Q}_h = 75$ W (above threshold), and the effect of the phase-shift ϕ applied to the feedback loop is observed for different values of the amplification gain G. As depicted in Fig. 3, the gradual increase of ϕ results in significant ("sinusoidal-like") variations of the overall efficiency η around η_0: for phase-shifts ϕ between 0° and 180°, η is lower than η_0, while $\eta \geq \eta_0$ for $\phi \in [180°, 360°]$, with an optimum value around $\phi_{opt} \simeq 270°$. The amplitude of those variations grows as the amplification gain G in the feedback loop is increased, as one would reasonably expect.

Moreover, for the highest amplification gain $G = 10$ depicted by filled triangles, one can observe an additional phenomenon. There appears a phase-shift domain $\phi_\sim \in [50°, 60°]$, where the influence of the feedback loop is

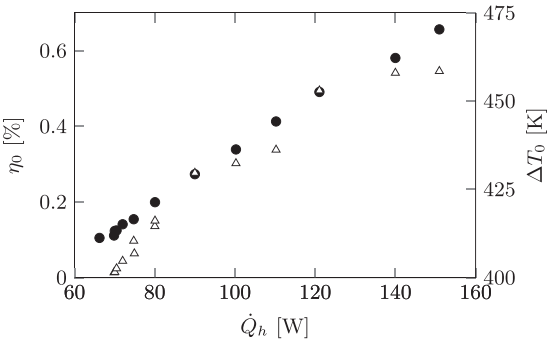

FIG. 2. Overall efficiency η_0 (•) of the engine and temperature difference ΔT_0 (△) through the regenerator when the auxiliary source is not powered, for various input heat powers $\dot{Q}_h$ above the onset threshold. The drive ratio (ratio of the amplitude of the acoustic pressure measured by the microphone μ to the static pressure P_0) varies correspondingly from 1% to 3.2%. These are the reference efficiency and temperature difference for the later comparison with the effect of the active control loop.

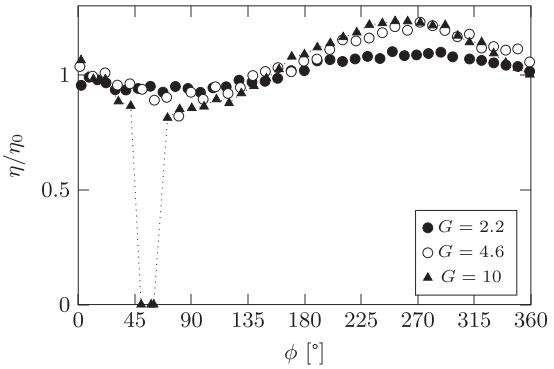

FIG. 3. Evolution of the efficiency η of the system as a function of the phase-shift ϕ for various amplification gains G at fixed input heat power $\dot{Q}_h = 75\,\mathrm{W}$, compared to the efficiency η_0 of the engine when the feedback loop present but is not powered ($\eta_0|_{\dot{Q}_h=75\,\mathrm{W}} \simeq 1.4 \times 10^{-3}$). Note the points corresponding to the death of the oscillation, for which $\eta = 0$. The dotted line is a guide for the eye.

such that it causes the death of the oscillations, as shown by the zero-efficiency points in Fig. 3. For this configuration, the amplitude of the self-sustained acoustic wave in the engine slowly decreases until the oscillations totally fade out. The engine then remains in this untriggered state. To set it back on, the power of the auxiliary source has to be shut off ($G = 0$), or the phase-shift needs to be modified to a value $\phi \neq \phi_\sim$.

B. Effect of phase-shift ϕ at fixed amplification gain G for various input heat powers $\dot{Q}_h$

Next, the amplification gain of the voltage applied to the auxiliary source is fixed to an intermediate value $G = 3.2$, and the effect of the phase-shift ϕ in the feedback loop is observed for various input heat powers $\dot{Q}_h$. For the highest input heat power $\dot{Q}_h = 80\,\mathrm{W}$, as depicted in Fig. 4(a) with triangles, the gradual increase of ϕ results in variations of the efficiency, which are similar to those depicted in Fig. 3. However, for the lowest heat powers $\dot{Q}_h = 70$ and $71\,\mathrm{W}$ marked with bullet points and open circles, respectively, the influence of ϕ on η is stronger. The improvement of the overall efficiency reaches values over 25%.

The death of the oscillations is observed here too. The closer the input power is to the onset threshold, the more the interval enlarges for which the acoustic wave is annihilated. For the lowest input heat power $\dot{Q}_h = 70\,\mathrm{W}$, which is just above the onset threshold, the phase-shift domain corresponding to oscillation death extends to almost half of the phase range, $\phi_\sim \in [10°, 140°]$.

It is also instructive to observe the evolution of the temperature difference in the regenerator in the same conditions, which is presented in Fig. 4(b). The results show that, as the efficiency is improved ($\phi > 180°$), the temperature difference in the regenerator is lowered, while ΔT rises as the feedback loop makes the efficiency decrease. Such a result enlightens the coupling between the acoustic field in the engine and the temperature distribution in the TAC and, notably, the fact that an increase of the produced acoustic power leads to a decrease of ΔT due to an increase of heat transport by sound within the TAC. Also, in the case of

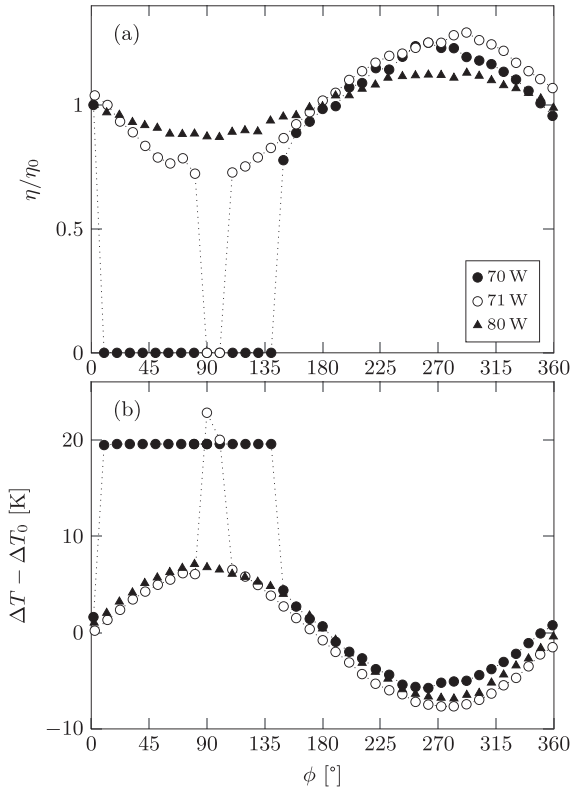

FIG. 4. (a) Evolution of the overall efficiency η as a function of the phase-shift ϕ for different heat powers $\dot{Q}_h$ at fixed amplification gain $G = 3.2$, compared to the efficiency of the engine when the feedback loop is not powered. (b) Corresponding evolution of the temperature difference ΔT in the regenerator, compared to the temperature difference ΔT_0 when the feedback loop is not powered. The dotted lines are guides for the eye.

oscillation death, the temperature difference rises to reach a limit value $\Delta T_\sim$ significantly larger than the temperature difference ΔT_0 corresponding to steady-state operation above threshold without active control ($G = 0$). This result supports the fact that without thermoacoustic energy conversion, the temperature field is only controlled by thermal diffusion (and possibly free convection) through the TAC.

C. Effect of the gain G for an optimal phase-shift ϕ_{opt}

Now, the phase-shift is fixed around its optimum value $\phi_{opt} \simeq 270°$, maximizing the efficiency improvement. The effect of increasing the voltage gain G is investigated, for two different input heat powers $\dot{Q}_h = 70$ and $150\,\mathrm{W}$. The variations of efficiency of the system are presented in Fig. 5.

In the case of a low input heat power ($\dot{Q}_h = 70\,\mathrm{W}$, just above threshold), depicted by circles, the maximum power $\dot{W}_{LS,max} \simeq .5\,\mathrm{W}$ supplied to the auxiliary source for $G = 10$ is small compared to the heat power $\dot{Q}_h$. The increase of output power generated thanks to the active control is then of greater influence in the estimation of η, as given by Eq. (2). However, in the case of the high input heat power $\dot{Q}_h = 150\,\mathrm{W}$, depicted with triangles in Fig. 5, the reference efficiency $\eta_0|_{150\,\mathrm{W}}$ is much larger ($\eta_0|_{150\,\mathrm{W}} > 7\eta_0|_{70\,\mathrm{W}}$, see Fig. 2). Therefore, because the electric voltage supplied to the auxiliary source is proportional to the acoustic pressure within the device, $\dot{W}_{LS}$ takes greater values (up to 8 W for

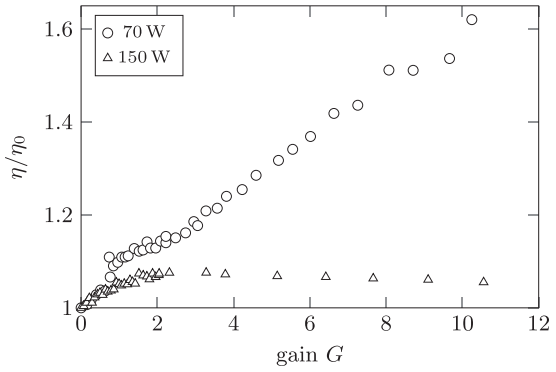

FIG. 5. Evolution of the overall efficiency η with the amplification gain G in the electroacoustic feedback loop, for two different input heat powers $\dot{Q}_h$, and for the phase-shift maximizing the increase of efficiency $\phi = \phi_{opt}$, compared to the efficiency of the engine when the feedback loop is not powered. η_0 is to be found in Fig. 2.

$G = 10$), which are not small anymore compared with $\dot{Q}_h$. As a result, and though the active control still generates an increase of the output power, the required power in the auxiliary source is so important that it leads to a saturation in the increase of the efficiency for values of the gain around $G_{sat} \simeq 2.5$, and even a decrease of the efficiency for higher values of $G > G_{sat}$.

In Fig. 6, the increase of the outgoing power generated when the active control is switched on, $\Delta\dot{W}_{el} = \dot{W}_{el} - \dot{W}_{el0}$ is compared to the power W_{LS} necessary to drive the auxiliary source, under the same experimental conditions as in Fig. 5. Comparing $\Delta\dot{W}_{el}$ to W_{LS} is indeed a good way to evaluate the applicability of the electroacoustic feedback loop, because if the former ($\Delta\dot{W}_{el}$) exceeds the latter (W_{LS}), then the net result of the active control is positive. This situation is observed in both cases presented in Fig. 6, at least for low values of the voltage gain G: for $\dot{Q}_h = 70$ W, the power balance is positive until $G = 1.5$, while for $\dot{Q}_h = 150$ W, the balance is positive up to $G \leq 0.3$.

IV. DISCUSSION AND CONCLUSION

From the results of the experimental study presented in Sec. III, it appears that the use of a single auxiliary source

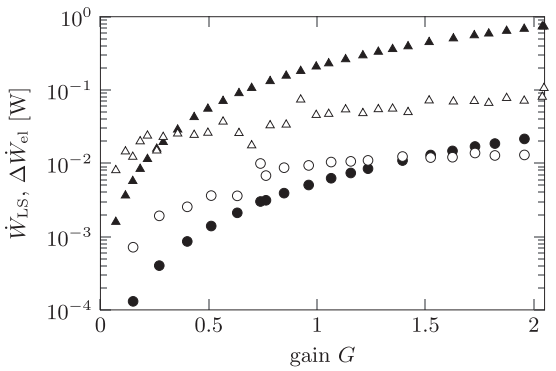

FIG. 6. Comparison of the increase of the outgoing power $\Delta\dot{W}_{el}$ generated when the active control is switched on (open symbols ○,△) to the power used to drive the electroacoustic feedback loop $\dot{W}_{LS}$ (filled symbols ●,▲) for various amplification gains G and two different input heat powers (○, ●: $\dot{Q}_h = 70$ W; △,▲: $\dot{Q}_h = 150$ W). If the open symbols are higher than the corresponding filled symbols, the additional output power produced thanks to active control is greater than the power supplied to the auxiliary source.

powered by a feedback loop is a promising technical solution to control the thermoacoustic conversion efficiency of a thermoacoustic engine, and thereby to increase the overall efficiency of the engine. The effect of the electroacoustic feedback loop has been shown to be potentially advantageous (in terms of performance improvement) when the thermoacoustic engine is operated slightly above the onset of self-sustained oscillations. Moreover, by showing the decrease of the temperature difference in the regenerator as the efficiency increases (see Fig. 4) in the presence of active control, it has been shown that an increase of output power can be accompanied with a decrease of the operating temperature difference ΔT. Such an information is highly pertinent for the development of systems powered from waste heat recovery, where the low temperature of the hot heat exchanger (typically up to around 550 K) is a strong constraint. However, some aspects of this experimental study are open to criticism before to draw further conclusions.

The first aspect deals with the physical interpretation of the results presented in Sec. III. The nonlinear coupling between the auxiliary sound source and the thermoacoustic auto-oscillator has been clearly brought out, as demonstrated notably by the phenomenon of oscillation death. However, the physical explanation about why and how the feedback loop can impact the thermoacoustic energy conversion is not perfectly clear. The simplest possible explanation would be that the thermoacoustic oscillator is forced to lock to the phase difference imposed between the loudspeaker and the reference microphone, which leads to the modification of the acoustic field in the whole device, and more specifically within the regenerator. As a result, the thermoacoustic amplification process would be modified, leading to additional amplification or attenuation (depending on the assigned phase-shift ϕ). However, complementary explanations are also possible, like the indirect (i.e., acoustically induced) modification of the *shape* of the temperature field within the TAC induced, for instance, by a change in the acoustic streaming pattern. It is indeed worth mentioning that the thermoacoustic amplification is not only controlled by the temperature difference between the two main heat exchangers, but also by the details of the temperature distribution within the TAC (including the TBT),[34] the latter being partly controlled by the acoustic field, which itself might be significantly modified in the presence of the electroacoustic feedback loop.

The second aspect deals with the (linear and nonlinear) coupling of the thermoacoustic oscillator with the auxiliary sound source. Here, the choice of an enclosed loudspeaker as the auxiliary source is the result of a technical compromise between the ease of implementation, the acoustic power delivered by the source and the impact of the source addition on the performance of the system without active control ($G = 0$). As pointed out in Sec. II, the choice made here is not the best since the highest achievable efficiency using active control is at best the same as the one reached when the feedback loop is totally removed from the device. Indeed this engine was initially designed (and optimized) without the auxiliary source and adding the active control loop unfortunately impacts its operation. The enclosed

loudspeaker amounts to a mass-spring oscillator coupled to the device, with subsequent variations of its resonant properties. Using instead an acoustic source with an infinite mechanical impedance (e.g., a rigid piston driven through a Scotch yoke mechanism) should fix the problem of the coupling between the source and the thermoacoustic oscillator, and it could even potentially increase the efficiency as soon as the source is switched on. Also, another way to fix the problem could be to account for the influence of the auxiliary source during the early design stage of the complete engine, which would allow at least to minimize the onset threshold of thermoacoustic oscillations.

The two open questions mentioned above are therefore to be addressed, and future works will be devoted to complementary experimental studies as well as the development of an adequate modeling describing the forcing of thermoacoustic oscillations in this device.

[1]C. Sondhauss, Ann. Phys. **155**, 1 (1850).
[2]N. Rott, Adv. Appl. Mech. **20**, 135 (1980).
[3]P. H. Ceperley, J. Acoust. Soc. Am. **66**, 1508 (1979).
[4]J. Wheatley, T. Hofler, G. Swift, and A. Migliori, J. Acoust. Soc. Am. **74**, 153 (1983).
[5]G. W. Swift, J. Acoust. Soc. Am. **84**, 1145 (1988).
[6]S. Backhaus and G. W. Swift, Nature **399**, 335 (1999).
[7]S. Backhaus and G. W. Swift, J. Acoust. Soc. Am. **107**, 3148 (2000).
[8]S. Backhaus, E. Tward, and M. Petach, Appl. Phys. Lett. **85**, 1085 (2004).
[9]T. Yazaki, A. Tominaga, and Y. Narahara, J. Heat Transfer **105**, 889 (1983).
[10]S. Boluriaan and P. J. Morris, Int. J. Aeroacoust. **2**, 255 (2003).
[11]M. W. Thompson, A. A. Atchley, and M. J. Maccarone, J. Acoust. Soc. Am. **117**, 1839 (2005).
[12]M. W. Thompson and A. A. Atchley, J. Acoust. Soc. Am. **117**, 1828 (2005).
[13]S. Moreau, H. Bailliet, and J.-C. Valière, J. Acoust. Soc. Am. **125**, 3514 (2009).
[14]C. Desjouy, G. Penelet, P. Lotton, and J. Blondeau, J. Acoust. Soc. Am. **126**, 2176 (2009).
[15]G. Penelet, M. Guedra, V. Gusev, and T. Devaux, Int. J. Heat Mass Transfer **55**, 6042 (2012).
[16]H. Yuan, S. Karpov, and A. Prosperetti, J. Acoust. Soc. Am. **102**, 3497 (1997).
[17]V. Gusev, H. Bailliet, P. Lotton, and M. Bruneau, Acta Acust. Acust. **86**, 25 (2000).
[18]R. S. Wakeland and R. M. Keolian, J. Acoust. Soc. Am. **115**, 2071 (2004).
[19]G. W. Swift, *Thermoacoustics: A Unifying Perspective for Some Engines and Refrigerators* (Acoustical Society of America Publications, Sewickley, PA, 2002).
[20]M. Guedra, G. Penelet, P. Lotton, and J.-P. Dalmont, J. Acoust. Soc. Am. **130**, 145 (2011).
[21]F. C. Bannwart, G. Penelet, P. Lotton, and J.-P. Dalmont, J. Acoust. Soc. Am. **133**, 2650 (2013).
[22]W. C. Ward, G. W. Swift, and J. P. Clark, J. Acoust. Soc. Am. **123**, 3546 (2008).
[23]M. Guedra and G. Penelet, Acta Acust. Acust. **98**, 232 (2012).
[24]J. R. Olson and G. W. Swift, Cryogenics **37**, 769 (1997).
[25]M. E. H. Tijani and S. Spoelstra, J. Appl. Phys. **110**, 093519 (2011).
[26]A. Pikovsky, M. G. Rosenblum, and J. Kurths, *Synchronization: A Universal Concept in Nonlinear Sciences* (Springer, Berlin, 2001).
[27]W. Lauterborn, Acustica **82**, S46 (1996).
[28]P. S. Spoor and G. W. Swift, J. Acoust. Soc. Am. **108**, 588 (2000).
[29]G. Penelet and T. Biwa, Am. J. Phys. **81**, 290 (2013).
[30]T. Yoshida, T. Yazaki, Y. Ueda, and T. Biwa, J. Phys. Soc. Jpn. **82**, 103001 (2013).
[31]T. Yazaki, Phys. Rev. E **48**, 1806 (1993).
[32]C. Desjouy, G. Penelet, and P. Lotton, J. Appl. Phys. **108**, 114904 (2010).
[33]A. M. Fusco, W. C. Ward, and G. W. Swift, J. Acoust. Soc. Am. **91**, 2229 (1992).
[34]G. Penelet, V. Gusev, P. Lotton and M. Bruneau, Phys. Lett. A **351**, 268 (2006).